entropy

MDPI

Article

Application of Entropy-Based Metrics to Identify Emotional Distress from Electroencephalographic Recordings

Beatriz García-Martínez, Arturo Martínez-Rodrigo *, Roberto Zangróniz Cantabrana, Jose Manuel Pastor García and Raúl Alcaraz

Research Group in Electronic, Biomedical and Telecommunication Engineering, University of Castilla-La Mancha, Cuenca 16071, Spain; Beatriz.GMartinez@uclm.es (B.G.-M.); Roberto.Zangroniz@uclm.es (R.Z.G.); JoseManuel.Pastor@uclm.es (J.M.P.G.); raul.alcaraz@uclm.es (R.A.)
* Correspondence: arturo.martinez@uclm.es; Tel.: +34-969-17-91-00 (ext. 4862)

Academic Editor: Kevin H. Knuth
Received: 18 April 2016; Accepted: 30 May 2016; Published: 3 June 2016

Abstract: Recognition of emotions is still an unresolved challenge, which could be helpful to improve current human-machine interfaces. Recently, nonlinear analysis of some physiological signals has shown to play a more relevant role in this context than their traditional linear exploration. Thus, the present work introduces for the first time the application of three recent entropy-based metrics: sample entropy (SE), quadratic SE (QSE) and distribution entropy (DE) to discern between emotional states of calm and negative stress (also called distress). In the last few years, distress has received growing attention because it is a common negative factor in the modern lifestyle of people from developed countries and, moreover, it may lead to serious mental and physical health problems. Precisely, 279 segments of 32-channel electroencephalographic (EEG) recordings from 32 subjects elicited to be calm or negatively stressed have been analyzed. Results provide that QSE is the first single metric presented to date with the ability to identify negative stress. Indeed, this metric has reported a discriminant ability of around 70%, which is only slightly lower than the one obtained by some previous works. Nonetheless, discriminant models from dozens or even hundreds of features have been previously obtained by using advanced classifiers to yield diagnostic accuracies about 80%. Moreover, in agreement with previous neuroanatomy findings, QSE has also revealed notable differences for all the brain regions in the neural activation triggered by the two considered emotions. Consequently, given these results, as well as easy interpretation of QSE, this work opens a new standpoint in the detection of emotional distress, which may gain new insights about the brain's behavior under this negative emotion.

Keywords: EEG; distress; entropy-based measures; nonlinear analysis

1. Introduction

From a psycho-physiological point of view, emotions consist of mental processes characterized by a strong activity and high degree of hedonistic content [1]. Their study is highly interesting because they are present in a variety of daily human activities including learning, verbal and nonverbal communication and rational decision-making processes [1]. Moreover, although the recognition of emotions plays a key role in the communication and interaction among people, nowadays automatic systems are not completely able to interpret human feelings [2]. This dysfunction often makes current human-machine interfaces (HMIs) unable to execute proper emotion-based actions [2]. Hence, more research is essential to improve affective computing systems, which are becoming increasingly applied to growing fields such as medicine [3,4], digital society [5] or computer games [6].

A major problem for the identification of emotions is the lack of a standard model for their definition [7]. In fact, several theories attempting to classify numerous emotional states can be found in the literature. Thus, Ekman firstly defined six basic emotions universally accepted including happiness, surprise, sadness, fear, disgust and anger, their combination being also able to characterize more complex feelings [8]. For instance, a total of fifty-five emotions were described with this model in the HUMAINE Project [9]. However, nowadays, the most widely used emotion classification model is the two-dimensional approach proposed by Russell [10]. This model is based on how pleasant or unpleasant (valence) a stimulus is, as well as on its ability to produce excitement or calmness (arousal) on a normal subject. A wide range of emotions can then be defined depending on the combination of different levels of arousal and valence [10], such as can be seen in Figure 1.

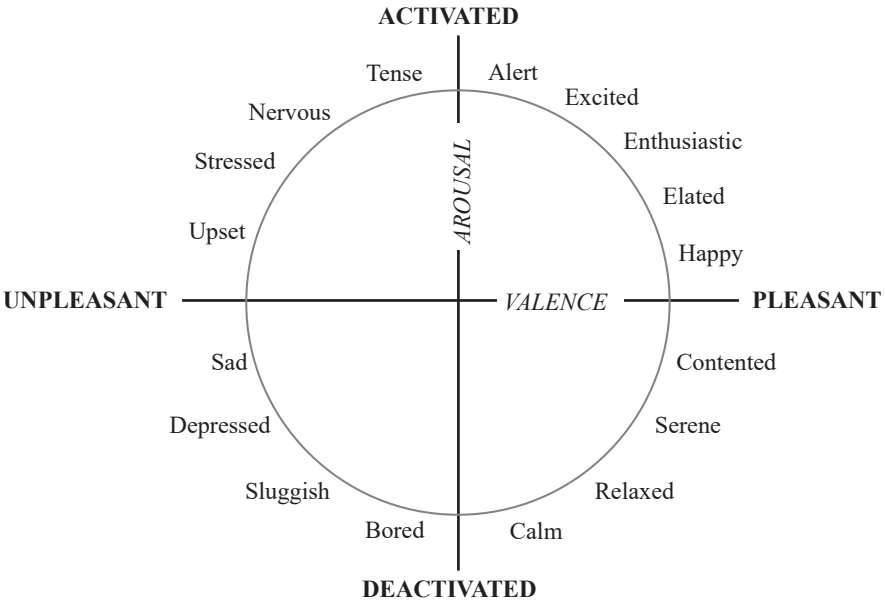

Figure 1. Graphical representation of the emotion classification model proposed by Russell [10].

Another relevant problem dealing with emotions is that they are highly intercorrelated. Thus, subjects rarely describe isolated positive or negative feelings [1]. Additionally, a stimulus can trigger different emotions within several people, mainly depending on their mood, personality, disposition or motivation [1]. Hence, this high variability in expression of emotions makes their automatic identification remain as a challenging task [7]. Nonetheless, some neurophysiological studies have suggested that most of emotions can lead to measurable changes in physiological activity [11]. Indeed, it has been mainly reported that the emotional state of a person can directly affect the arousal level of his nervous system [12]. Thus, some authors have tried to quantify objectively the physiological alterations triggered by different emotions. With respect to this, voice and facial expressions have been widely analyzed [11]. However, these physical features vary across cultures and nationalities and, therefore, they are unable to recognize emotions successfully in a universal way [13]. In contrast, a more general and objetive identification of emotions has been reached from the analysis of some physiological signals, such as the electrocardiogram (ECG), the electromyogram (EMG) or the electro-dermal activity (EDA) [7]. However, the methods' performance dealing with these recordings is still far from being optimal to be included in HMIs [7].

Within this context, the identification of emotions from electroencephalographic (EEG) recording has recently begun to be explored because it may give more valuable information than other physiological signals [14]. In fact, whereas the brain is the primary response source to any external stimulus, other physiological signals can only capture the subsequent secondary processes generated by this organ [14]. With respect to this, novel methods to quantify functional connectivity among

different brain areas have been proposed with the aim of discovering new insights about the brain's response to different emotional processes [15,16]. Thus, these algorithms have been used to identify different emotions elicited by audiovisual stimuli [16–18], as well as to characterize mental disorders, such as major depression [19,20], consciousness problems [21], epilepsy [22], Alzheimer's [23] or schizophrenia [24].

Additionally, numerous works have also shown a greater usefulness of the nonlinear analysis of several physiological signals compared to their traditional linear exploration [7]. However, no rigorous studies in this respect have been conducted from single EEG channels [14,25]. Therefore, the main goal of the present work is to analyze the ability of three novel entropy-based measures, *i.e.*, sample entropy (SE), quadratic SE (QSE) and distribution entropy (DE), to identify some emotions from the EEG signals. It is interesting to note that non-linearity in the brain is introduced even at the cellular level, since the dynamical behavior of individual neurons is governed by threshold and saturation phenomena [26]. More globally, the brain also presents a really complex and heterogeneous performance, which makes its behavior far from being considered linear [27]. Hence, the use of entropy-based metrics in the described context is completely justified. Indeed, these kinds of indices have already shown an interesting ability to reveal useful clinical information in mental disorders, such as Alzheimer's [26,28,29], epilepsy [30] or depression [31].

In the last few years, an emotion receiving increasingly attention is negative stress (also called distress), since it is a major problem in developed countries [32,33]. In fact, typical factors in the current lifestyle of those countries, such as competitiveness, social judgement, productivity demands or information overload, lead many people to a frenetic rhythm [33]. This emotion has been defined as the change from a state of calm to another of excitement to preserve the integrity of the organism [32,34]. Moreover, it has been assessed in a wide variety of scenarios, including driving tasks [34], military exercises [35], surgical procedures [36] and online exams [37]. A recent study has also quantified negative stress in elderly who decide to stay at home to prevent major depression [38]. Although short-term distress may not be a risk factor for health, chronic negative stress can result in mental diseases like generalized anxiety or depression [39]. Moreover, this emotion can sometimes represent a risk factor for hypertension and coronary artery disease [40] as well as cause or aggravate other physical disorders, such as irritable bowel syndrome, gastroesophageal reflux disease or back pain [41,42]. As a consequence, the present work is completely focused on discerning between the emotional states of calm and negative stress.

The remainder of the paper is organized as follows. Section 2 describes the used database, the entropy-based metrics computed from the EEG recording as well as the developed statistical study. Section 3 summarizes the obtained results, which are next discussed in Section 4. Finally, Section 5 presents concluding remarks.

2. Methods

2.1. Database

The freely available Database for Emotion Analysis using Physiological Signals (DEAP) [43] was used in the present work. This dataset consists of 1280 EEG recordings corresponding to thirty-two healthy volunteers with ages between 19 and 37 years (50% men, mean age 26.9). In order to elicit different emotions, the subjects under study visualized forty, one minute-length, music videos with emotional content. Then, participants rated the videos in terms of valence and arousal by using self-assessment manikins (SAM). In these tests, intensity scales to quantify excitation and pleasure are represented by graphic pictures expressing nine levels [44]. During the process, EEG recordings were acquired at a sampling frequency of 512 Hz from 32 standard 10–20 system electrodes located over the scalp. To prepare the signals for further analysis, they were referenced making use of the typical Common Average Reference technique. In this approach, mean potential from all EEG channels is removed from each single electrode. The signals were also downsampled to 128 Hz and

band-pass filtered between 4 and 45 Hz. Moreover, eye blink artifacts were also removed by using an algorithm based on independent component analysis. Additional details about the database and EEG preprocessing can be found in [43].

Among all EEG recordings, only two subsets were chosen in order to validate the identification of negative stress obtained by the proposed entropy-based indices, such as Figure 2 shows. Both groups were selected according to previous works where the same problem was analyzed [45–47]. Thus, the group of calm subjects was composed of the samples with an arousal level lower than 4 and a valence level between 4 and 6. Similarly, the group of distressed individuals consisted of the samples with an arousal level higher than 5 and a valence level lower than 3. The total number of analyzed EEG recordings was 279, *i.e.*, 146 from calm subjects and 133 from distressed subjects. Finally, it is worth noting that only the last 30 s from each recording were analyzed, such as in previous works dealing with the same database [43].

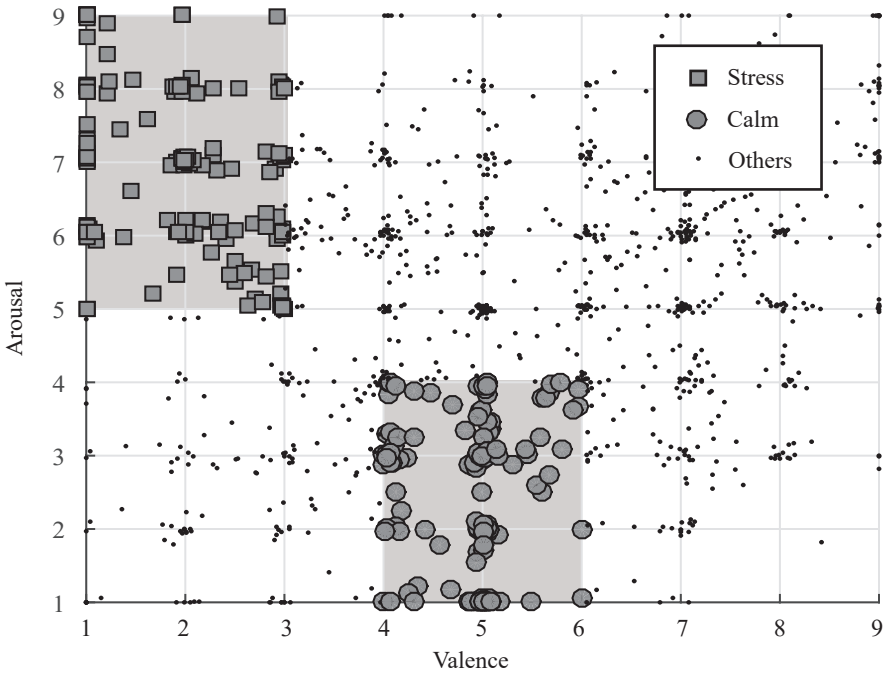

Figure 2. Distribution of the samples contained by the DEAP dataset within the valence–arousal space. Data chosen for study (*i.e.*, calm and distressed subjects) are clearly highlighted.

2.2. Description of Entropy-Based Metrics

Nonlinear analysis has proven to be valuable in the assessment of physiological time series because hidden information related to underlying mechanisms has been obtained in a wide variety of clinical scenarios [48]. Nonetheless, although a high amount of nonlinear measures exist, entropies based on quantifying time series regularity have been widely used in the last few years since they can work successfully even with short and noisy recordings [49]. Indeed, approximate entropy (AE) and its improved version SE are extensively known metrics, which examine a time series for similar epochs and assign a non-negative number to the sequence, with larger values corresponding to more irregularity in the data [50].

From a formal point of view, given N data points for a time series $x(n) = \{x(1), x(2), \ldots, x(N)\}$, SE can be defined as follows [50]:

1. Form vector sequences of size m, $\mathbf{X}_m(1), \ldots, \mathbf{X}_m(N-m+1)$, defined by $\mathbf{X}_m(i) = \{x(i), x(i+1), \ldots, x(i+m-1)\}$, for $1 \leq i \leq N-m$. These vectors represent m consecutive x values, starting with the ith point.

2. Define the distance between vectors $\mathbf{X}_m(i)$ and $\mathbf{X}_m(j)$, $d[\mathbf{X}_m(i), \mathbf{X}_m(j)]$, as the absolute maximum difference between their scalar components,

$$d[\mathbf{X}_m(i), \mathbf{X}_m(j)] = \max_{k=0,\ldots,m-1} \Big(|x(i+k) - x(j+k)| \Big). \tag{1}$$

3. For a given $\mathbf{X}_m(i)$, count the number of j ($1 \leq j \leq N-m$, $j \neq i$), denoted as B_i, such that the distance between $\mathbf{X}_m(i)$ and $\mathbf{X}_m(j)$ is less than or equal to r. Then, for $1 \leq i \leq N-m$,

$$B_i^m(r) = \frac{1}{N-m-1} B_i. \tag{2}$$

4. Define $B^m(r)$ as

$$B^m(r) = \frac{1}{N-m} \sum_{i=1}^{N-m} B_i^m(r). \tag{3}$$

5. Increase the dimension to $m+1$ and calculate A_i as the number of $\mathbf{X}_{m+1}(i)$ within r of $\mathbf{X}_{m+1}(j)$, where j ranges from 1 to $N-m$ ($j \neq i$). Then, $A_i^m(r)$ is defined as

$$A_i^m(r) = \frac{1}{N-m-1} A_i. \tag{4}$$

6. Set $A^m(r)$ as:

$$A^m(r) = \frac{1}{N-m} \sum_{i=1}^{N-m} A_i^m(r). \tag{5}$$

Thus, $B^m(r)$ is the probability that two sequences will match for m points, whereas $A^m(r)$ is the probability that two sequences will match for $m+1$ points. Finally, SE can be defined as

$$SE(m, r) = \lim_{N \to \infty} \Big\{ -\ln \Big[\frac{A^m(r)}{B^m(r)} \Big] \Big\}, \tag{6}$$

which is estimated by the statistic

$$SE(m, r, N) = -\ln \Big[\frac{A^m(r)}{B^m(r)} \Big]. \tag{7}$$

Although m and r are critical in determining the outcome of SE, no guidelines exist for optimizing their values. In principle, the accuracy and confidence of the entropy estimate improve as the number of length m matches increase. The number of matches can be increased by choosing small m (short templates) and large r (wide tolerance). However, penalties appear when too relaxed criteria are used [49]. For smaller r values, poor conditional probability estimates are achieved, while for larger r values, too much detailed system information is lost and SE tends to 0 for all processes. A slight modification of SE that makes it insensitive to the r selection is the named QSE [51]. This measure allows r to vary as needed to achieve confident estimates of the conditional probability and is defined as

$$QSE(m, r, N) = SE(m, n, r) + \ln(2r). \tag{8}$$

The most widely established values m and r for computation of these entropies are $m = 1$ or $m = 2$ and r between 0.1 and 0.25 times the standard deviation of the original time series [52]. Normalizing r in this manner gives, both to SE and QSE, a translation and scale invariance, in the sense that they remain unchanged under uniform process magnification, reduction, or constant shift to higher or lower values [52]. According to several previous works dealing with EEG recordings, SE and QSE were here estimated using $m = 1$ and $r = 0.15, 0.25$ and 0.30 times the standard deviation of $x(n)$ [53]. Note that three values of r were considered to evaluate the effect of this parameter on the entropy estimates.

Despite the usefulness proved by both SE and QSE to reveal clinical information in many contexts, some previous works have also noticed that they are only able to quantify a time series irregularity, thus sometimes misinterpreting its real complexity [54,55]. Indeed, time series irregularity can increase with the degree of randomness and, in this case, the increase in SE or QSE may not be necessarily indicative of an increase in complexity [55]. One reason for this issue may be the fact that these metrics do not take into consideration the multiple temporal scales inherently presented by complex dynamics [54,55]. To overcome this problem, Costa *et al.* [54] proposed a multi-scale approach based on computing SE from several time scales and then obtaining their average. However, this metric requires larger time series than SE and QSE to obtain robust results [54]. More recently, Li *et al.* [55] have proposed an alternative solution based on computing spatial information from the distance matrix among m-length patterns. Thus, the metric named DE is able to quantify complexity of times series as short as those required by SE and QSE [55].

As for SE and QSE, the first step to compute DE is to form $N - m$ vectors of m samples in length. Then, the distance matrix $\mathbf{D} = \{d[\mathbf{X}_m(i), \mathbf{X}_m(j)]\}$, for all $1 \leq i, j \leq N - m$, and its empirical probability density function can be considered as a histogram of M bins. To reduce bias, elements with $i = j$ are excluded and DE is then computed as:

$$DE(m, M) = -\frac{1}{\log_2(M)} \sum_{k=1}^{M} p_k \log_2(p_k), \tag{9}$$

p_k being the probability of each bin. Note that DE is normalized and, therefore, it can only range from 0 to 1 for one-peak and fully flat probability density functions of $\mathbf{D}$, respectively. Moreover, because a base-2 algorithm is used, M should be chosen as an integer power of 2. Nonetheless, the selection of this value is not as critical as the selection of r in SE. Indeed, every relatively large value of M can successfully quantify distribution of $\mathbf{D}$. According to the authors' recommendation [55], values of $M = 512$ and $m = 2$ were used in the present study.

2.3. Statistical Analysis

Shaphiro–Wilks and Levene tests proved that distributions of SE, QSE and DE were normal and homoscedastic for all the EEG channels. Consequently, results are expressed as mean $\pm$ standard deviation (std) for all the samples belonging to the same group and statistical differences between emotional states of calm and distress were assessed by a Student's t-test. A value of statistical significance $\rho < 0.05$ was considered as significant.

In order to assess the discriminant ability of each metric, two different approaches were considered. Firstly, all the EEG recordings were jointly considered and a tenfold stratified cross-validation was used. This kind of cross-validation allows for obtaining a highly reliable performance generalization of the metric under study [56]. Indeed, this approach makes use of all the available data both for training and testing, thus avoiding the problem that classification results could be highly dependent on the choice for a training-test split. Precisely, the database was first partitioned into 10 equally sized fold, rearranging the data to ensure that each fold is a good representative of the whole. Subsequently, 10 iterations of training and validation were performed, such that within each one, a fold of the data was held out for validation, whereas the other ones were used for learning. For each learning set, a receiver operating characteristic (ROC) curve was used to obtain the optimal discriminant threshold between calm and distressed subjects. The ROC is the result of plotting the fraction of true positives out of positives (*i.e.*, sensitivity) against the fraction of false positives out of negatives (*i.e.*, 1−specificity) at various threshold settings. Sensitivity was here considered as the percentage of stressed subjects correctly classified, whereas the rate of calm individuals properly identified was considered as specificity. The optimal threshold was selected as that one providing the highest accuracy, *i.e.*, the highest number of subjects correctly classified. At the end, accuracy was also obtained for the test fold and averaged for the 10 iterations.

On the other hand, to evaluate the effect of the inter-individual variability on the cross-validated discriminant ability obtained for each metric, a subject-related classification was also carried out. Thus, the mean classification threshold resulting from the cross-validation approach was used to classify the samples from each single subject, and average values of sensitivity, specificity and accuracy for all individuals in the database were finally computed.

Additionally, the relationships among the nonlinear dynamics quantified from the different brain areas were analyzed by means of decision trees and fuzzy rules. Thus, several optimal combinations of the SE, QSE and DE values obtained from all the EEG channels were first considered under study. Note that the growth of every tree was always stopped when any node only contained samples from a group of subjects or less than 20% of all samples. Moreover, every node was split by using an impurity-based Gini index [57]. It is also mandatory to mention that the effect of a dimensionality reduction approach, such as analysis of principal component analysis (PCA) [58], on the classification result was also explored from this kind of classifier. Thus, an experiment feeding a decision tree with the first principal components explaining 95% of variability in entropy values for all EEG channels was developed. Nonetheless, a well-known limitation of tree-based classifiers is the use of highly strict decision thresholds. Thereby, classification based on lighter fuzzy rules was also considered. In this case, for each input variable, two membership functions were built making use of a Gaussian distribution curve. The slopes and widths of each membership function were computed with a neuronal network, such that half of the samples were used as a training set and the remaining ones as a test group.

3. Results

The three considered entropies were computed for non-overlapped segments of $N = 640$ samples, such that their final values for each subject were obtained from the average of six segments. Although statistically significant differences among SE values were computed for $r = 0.15, 0.25$ and 0.30 were noticed, in no case were emotional states of calm and distress successfully discerned. A similar result was also obtained for DE and, consequently, Table 1 only shows classification outcomes yielded by QSE. As expected, in this case, no statistically significant differences between QSE values computed for the three different thresholds r were observed. Thus, this table only presents information about QSE values obtained for $r = 0.25$. In the interest of clearness, the table has been divided into two parts to display EEG channels separately from left and right brain hemispheres. Moreover, EEG channels have been sorted from front to back for each hemisphere.

Interestingly, most of the EEG channels (27 out of 32) showed statistically significant differences between both emotional states (see first column, Table 1). Although they belong to several brain areas, including frontal, central, parietal, temporal and occipital regions, it is interesting to note that the most remarkable differences were noticed in parietal channels $CP1$, $CP2$ and $P4$. Nonetheless, temporal channel $T7$ and frontal channels $F3$ and $AF4$ also reported highly relevant differences between both emotions. Another relevant observation is that QSE provided higher values for stressed subjects than for calm individuals from all the EEG channels, such as can be visually observed from Figures 3 and 4. Moreover, it is also worth highlighting that frontal, temporal, right parietal and left occipital areas presented more irregular dynamics for both emotional states than the remaining brain regions.

Table 1. Results obtained from QSE. Mean and std values for emotional states of calm and *negative* stress, statistical significance (ρ), sensitivity (Se), specificity (Sp) and accuracy (Ac) for all EEG channels are presented.

Hemisphere	EEG	Significance	Global Analysis			Subject-Related Analysis		
(L)eft/(R)ight	Channel	Value, ρ	Se (%)	Sp (%)	Ac (%)	Se (%)	Sp (%)	Ac (%)
L	$Fp1$	0.006	47.72	67.16	57.89	66.84	60.58	60.31
L	$AF3$	0.0021	59.06	61.80	60.50	60.88	63.79	60.16

Table 1. *Cont.*

Hemisphere	EEG	Significance	Global Analysis			Subject-Related Analysis		
(L)eft/(R)ight	Channel	Value, ρ	Se (%)	Sp (%)	Ac (%)	Se (%)	Sp (%)	Ac (%)
L	*F*3	7.11×10^{-5}	58.46	67.80	63.35	61.94	59.10	59.30
L	*F*7	> 0.05	60.24	42.91	51.88	53.64	63.90	55.35
L	*FC*5	0.0307	32.66	81.84	58.40	48.16	53.56	50.43
L	*FC*1	> 0.05	38.17	67.42	54.30	41.79	51.77	45.00
L	*C*3	0.038	27.75	77.46	53.77	42.28	49.49	47.45
L	*T*7	7.88×10^{-5}	56.34	61.77	59.17	67.57	67.68	64.46
L	*CP*5	> 0.05	27.26	78.52	54.05	41.70	63.36	54.71
L	*CP*1	1.55×10^{-6}	47.28	78.57	63.66	68.98	68.69	65.18
L	*P*3	0.0048	41.30	67.60	55.05	49.88	51.07	51.63
L	*P*7	0.0003	50.26	71.71	61.49	72.24	66.30	66.35
L	*PO*3	0.0205	25.81	83.49	55.99	49.50	45.43	50.03
L	*O*1	0.0132	54.18	55.89	55.09	66.84	55.13	61.64
L	*Oz*	0.002	49.79	71.39	61.09	66.91	60.20	60.68
L	*Pz*	0.0123	40.42	71.34	56.60	53.04	57.53	54.82
R	*Fp*2	0.0008	67.10	49.41	57.83	64.27	59.16	60.52
R	*AF*4	1.60×10^{-5}	62.51	61.58	62.05	71.24	71.81	67.40
R	*Fz*	0.0023	55.32	64.20	59.93	68.31	62.25	62.68
R	*F*4	0.0062	31.66	78.86	56.35	52.60	56.53	55.97
R	*F*8	0.0233	43.16	73.64	59.11	55.66	59.25	57.06
R	*FC*6	0.0325	40.30	72.06	56.91	67.81	62.81	63.09
R	*FC*2	> 0.05	54.06	62.32	58.38	59.69	52.99	55.66
R	*Cz*	0.001	57.28	61.14	59.25	65.04	70.46	64.85
R	*C*4	0.035	53.73	63.14	58.67	63.39	66.77	60.69
R	*T*8	0.0003	64.59	56.03	60.11	65.40	66.47	61.62
R	*CP*6	0.0088	48.56	62.46	55.80	66.88	65.36	63.14
R	*CP*2	4.25×10^{-6}	67.24	57.09	63.71	72.97	73.71	68.54
R	*P*4	3.86×10^{-7}	52.69	82.94	68.52	85.38	78.04	76.49
R	*P*8	0.0002	63.10	64.04	63.59	71.83	69.26	65.91
R	*PO*4	0.0009	53.31	64.39	59.11	60.79	56.75	59.47
R	*O*2	> 0.05	31.30	71.14	52.16	49.62	48.78	49.95

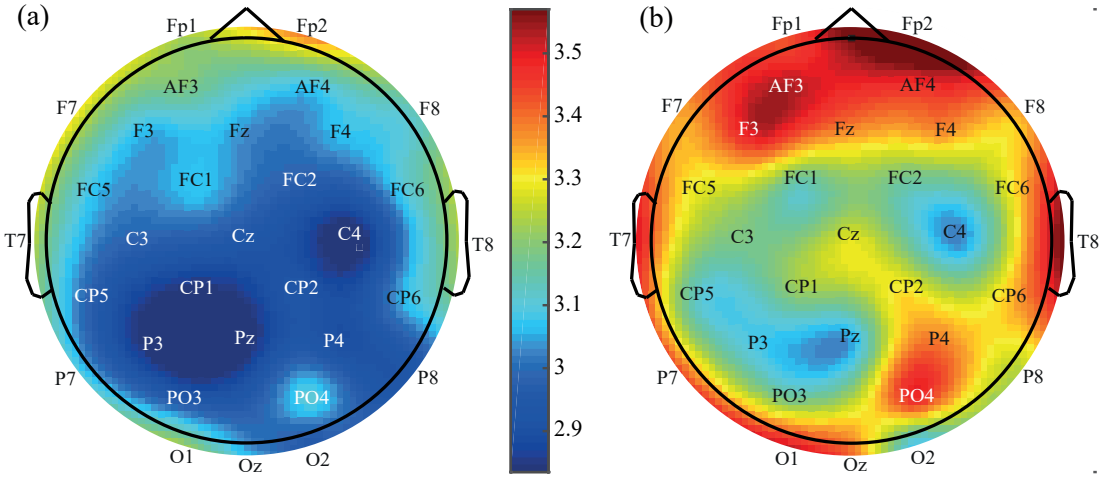

Figure 3. Graphical representation of average QSE values obtained from all EEG channels for (**a**) calm and (**b**) distressed subjects.

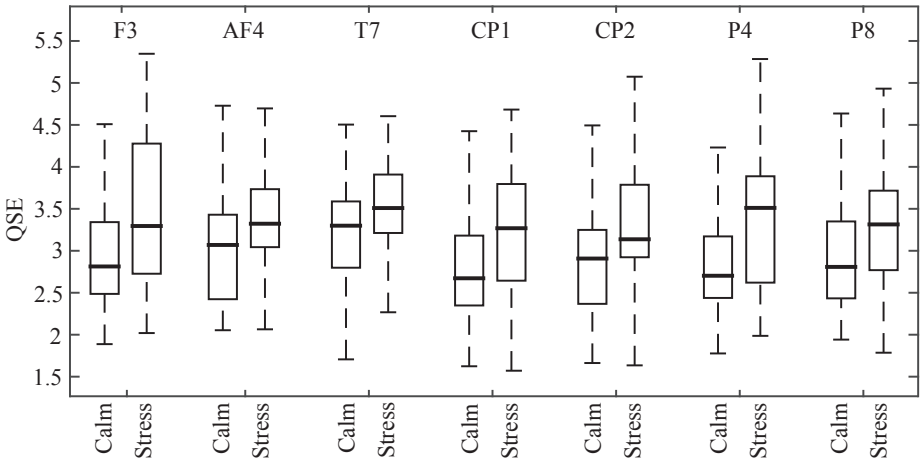

Figure 4. Boxplots of QSE values for emotional states of calm and distress obtained from the most statistically significant EEG channels.

Classification outcomes for the two considered analyses are also presented in Table 1. Thus, average values of sensitivity, specificity and accuracy obtained from stratified tenfold cross-validation are displayed by the columns labeled "Global Analysis". On the other hand, the last columns show results for the subject-related classification. In this case, mean values of sensitivity, specificity and accuracy for the 32 individuals under study are presented. In general, results for both cases are in agreement with the aforementioned statistical differences between emotional states. Indeed, the right parietal channel $P4$ provided the highest discriminant ability between calm and stressed subjects. Moreover, parietal and central-parietal channels $P8$, $CP1$ and $CP2$ as well as frontal channels $F3$ and $AF4$ also reported notably high values of diagnostic accuracy. Nonetheless, it is worth noting that differences between diagnostic accuracies for both cases were notably limited, thus ranging from 0.34% to 9.3% with a mean value of 3.77% $\pm$ 2.54%. However, apart from $F3$, EEG channels providing the highest statistical differences between both emotional states presented a higher discriminant ability for subjected-related classification than when all the data were considered together. For instance, QSE values for the channel $P4$ provided an accuracy increase from 68.52% to 76.49%. Nonetheless, for other channels, the accuracy got worse, thus even reaching values slightly lower than 50%.

In view of these outcomes, two tree-based classification models were considered to study the possible relationships among EEG channels. Thus, QSE values were only used to obtain a first discriminant model. The resulting two-level classifier combined the channels $P4$ and $O1$, such as Figure 5a displays. As expected, the most statistically significant channel $P4$ was initially used to identify the group of stressed subjects by means of the highest QSE values. The remaining individuals were classified by considering the regularity in the left occipital area (channel $O1$). Thus, in this case, the fact that this brain region presented more irregular dynamics for calm subjects than for stressed individuals was used to discern between both emotional states. In this way, considering jointly all of the data, the discriminant model improved diagnostic accuracy of $P4$ more than 3.5% because it yielded values of sensitivity, specificity and accuracy of 80.34%, 63.22% and 72.17%, respectively. Note that although specificity was slightly reduced regarding the classification reported by $P4$, sensitivity was increased around 18%. It is also interesting to highlight that when the classifier was redesigned by only considering the ten first principal components explaining 95% of variability, a very similar accuracy of 73.12% was also obtained. Nonetheless, in this case, more balanced values of sensitivity and specificity of 77.02% and 76.21%, respectively, were reported. Moreover, another relevant result was that no great differences in the contribution of all EEG channels to the considered principal components were observed. In fact, only maximum differences of around 3% were observed.

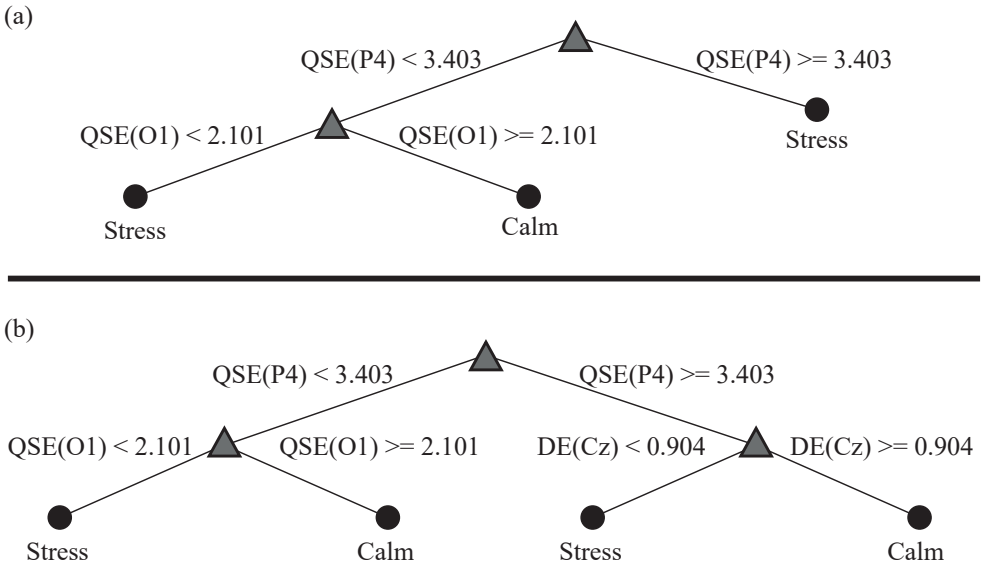

Figure 5. Tree-based discriminant models obtained by considering (**a**) only QSE values from all EEG channels and (**b**) SE, QSE and DE values from all EEG channels.

A second tree-based discriminant model was also constructed by considering values of SE, QSE and DE computed from all the EEG channels. In this case, a modified version of the classifier previously described was obtained, such as can be observed in Figure 5b. Indeed, only DE was additionally considered to obtain an improved discrimination between subjects presenting a highly irregular brain activity in the right parietal area (covered by *P*4). Thus, sensitivity and accuracy were improved around 7% and 3%, since the discriminant model reported values of sensitivity, specificity and accuracy of 87.49%, 62.18% and 75.29%, respectively.

Finally, it should be mentioned that results provided by tree-based classifiers were not improved by considering lighter decision thresholds via fuzzy rules. Indeed, the four fuzzy rules designed from QSE values for channels *P*4 and *O*1 only provided a diagnostic accuracy of 70.46%, with sensitivity and specificity values of 58.61% and 81.08%, respectively. Similarly, the eight fuzzy rules achieved from QSE values for channels *P*4 and *O*1 and DE values for the channel *Cz* were only able to reach a discriminant ability of 73.46%, with sensitivity of 61.13% and specificity of 81.63%.

4. Discussion

To the best of our knowledge, no thorough works exploring application of nonlinear analysis to the EEG recording for recognition of emotions can be found in the literature [14,25]. Thus, only a few studies have considered nonlinear indices, such as fractal dimension, correlation dimension or some entropy-based measures, to discern between emotional states of calm and negative stress [45–47]. Nonetheless, AE has revealed a promising ability to identify some emotions [59] and, therefore, the present work introduces for the first time the use of SE, QSE and DE to detect negative stress. These indices are improved versions of AE because SE was firstly designed to reduce the bias caused by including self-matches in its computation [50] and, more recently, QSE and DE have been proposed to resolve some SE issues. Precisely, QSE has been devised to reduce SE sensitivity to the threshold r [51], which has been here supported by the results presented for $r = 0.15, 0.25$ and 0.30, and DE to overcome SE limitation in the complexity estimation of times series [55].

Obtained outcomes have proven that only QSE is able to discern successfully between the two considered emotional states. Although this result could seem a bit surprising because SE and QSE are based on the same computation approach, QSE insensitivity to the threshold r plays a key role to obtain accurate estimates of times series regularity [51]. Indeed, in SE computation, r is habitually

normalized by original data standard deviation to avoid the effect of amplitude changes on the identification of similar patterns [49]. However, several authors have reported that this normalization is inappropriate to obtain precise regularity estimates in some cases [60–62]. For instance, if a time series presents quick and sudden amplitude changes, the standard deviation obtained from intervals of several seconds in length will not be useful to compute time series regularity from very short segments. Hence, QSE ability to estimate entropy and discard the effect of every amplitude change in time series could justify the different results obtained from both metrics. On the other hand, DE makes use of a very different computation approach from QSE and SE. Moreover, although time series normalization may notably influence entropy estimation, which might be responsible for the presented results, this aspect has not been analyzed by the authors who introduced recently the metric [55]. Therefore, this aspect will have to be addressed in a future work.

Although comparison among works should be considered with caution, since different ways to elicit emotions may trigger different cognitive processes [7], it is interesting to note that the present study has only shown a slightly poorer classification between emotional states of calm and distress than previous studies. Thus, whereas QSE values, both from single channels or their tree- and fuzzy-based combinations, have provided discriminant abilities between 70% and 75%, diagnostic accuracies around 80% have been previously reported [45–47]. However, it is mandatory to underline that these high discriminant rates have always been reached by combining dozens or even hundreds of features through advanced classifiers, such as support vector machines or neural networks [45–47]. Hence, the largest contribution of the present work is the introduction of a single entropy-based measure with a remarkable ability to discriminate between the two considered emotional states. In fact, the easy clinical interpretation of QSE may open a new standpoint in EEG-based identification of emotions, as well as provide new insights about the brain's behavior under different feelings.

It is also interesting to note that QSE combination with regularity and complexity levels measured from different brain areas has also improved its ability to identify negative stress. In this case, the obtained discriminant models, based both on decision trees or fuzzy rules, are still easily interpretable, since they only resulted in a few levels of classification (see Figure 5). Hence, they differ significantly from those proposed in previous works, where the clinical meaning of every single metric is blurred within the classification approach. Nonetheless, this later behavior has also been noticed when PCA was considered to exploit the redundant information from all EEG channels. Indeed, all the brain areas contributed in a very similar way to the principal components used for classification and, regrettably, no clear interpretations about their response to the emotional states of calm and distress could then be elucidated.

On the other hand, another interesting advantage of the present work is the higher spatial resolution considered to analyze the brain's behavior under negative stress. Thus, whereas most of previous works only studied a few EEG channels from the frontal area [45,46], regularity and complexity of all brain regions were here analyzed by considering 32 channels. This kind of analysis allows us to obtain a global vision about how this organ reacts to different emotional stimuli. With respect to this, Figure 3 shows that distressed individuals reported more irregular dynamics than calm subjects for the whole brain, thus suggesting a relevant neural activation during negative stress. This finding is in agreement with other previous neuroanatomy studies, which have provided that the brain secretes hormones, such as adrenaline or dopamine, into the bloodstream and directly in its cortex to intensify mental concentration [63]. Obviously, considering stress as a reaction to preserve organism's integrity, a concentration increase has mandatorily to occur during this emotion [34,63]. In addition, other previous works have also suggested a similar neural activation of most brain regions in subjects exposed to very distressfull [64] as well as chronic hyperarousal and post-traumatic experiences [65]. Similarly, a low and regular neuronal activity during an emotional state of calm has also been previously reported by works dealing with different relaxing therapies. Indeed, nonlinear indices like Lyapunov exponents or SE have been able to notice significant decreases in brain activation during relaxing music, foot reflexology and meditation [66,67].

Nonetheless, despite the general growth of neural activity during negative stress, it should also be highlighted that all brain regions did not provide the same behavior. With respect to this, Figure 6 shows how QSE differences from emotional states of calm and distress were especially relevant in the left frontal (channel *F*3) and right parietal (channel *P*4) areas. As before, this finding is consistent with previous works. Thus, Nitschke [68] reported a large asymmetry in neural activity under anxiety conditions, the left frontal area being the most active region. Moreover, in that study, a high brain activity in the right parietal area was also noticed during distress-inducing experiences [68]. In a similar way, Todder *et al.* [69] observed remarkable differences in the activity of right and left frontal areas for post-traumatic stress disorder (PTSD) patients and healthy subjects. More precisely, although a low-resolution electrical tomography was used, a higher activity in the left ventrolateral prefrontal brain cortex was noticed for PSTD patients than for controls. On the other hand, brain parietal areas have been associated with the arousal component of an emotion and frontocentral regions with both valence and arousal components [68,70].

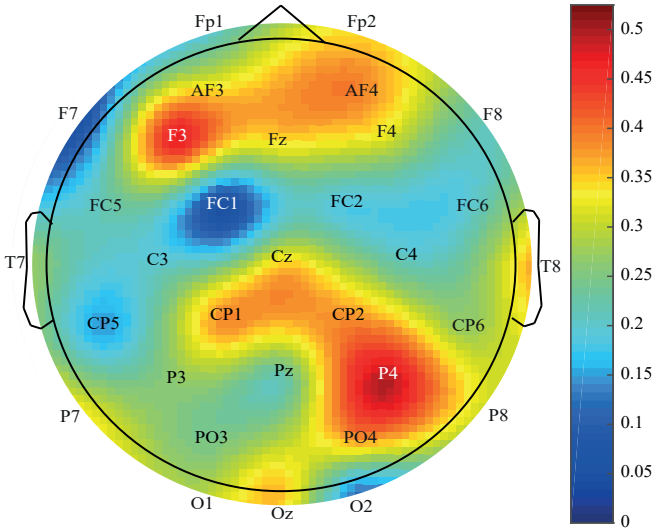

Figure 6. Graphical representation of the differences between QSE values for emotional states of calm and negative stress obtained from all EEG channels.

In view of this close agreement between previous clinical studies and the presented results, as well as the limited influence that has shown the inter-subject variability on the identification of calm and distressed individuals, it is worth considering that QSE's performance could be extrapolated to other datasets. Indeed, it has also been corroborated that the map of average QSE differences displayed by Figure 6 remains unaltered for most subjects in the database. Nonetheless, in order to confirm this assumption as well as evaluate the robustness of the presented results, further studies are required. With respect to this, connectivity analysis among brain areas by using nonlinear synchronization measures would also be very interesting to obtain new insights about the brain's response to different emotions. Moreover, it could also be useful to assess the possibility of discerning between positive and negative stress, since both feelings can cause a different impact on people's mood and health.

Finally, some comments about the analyzed DEAP dataset deserve consideration. Firstly, it was not created specifically to discern between emotional states of calm and negative stress and, indeed, many other emotions can be found (see Figure 2). Despite this and that international databases containing different kind of stimuli to elicit emotions exist and have been widely used to design tailored experiments [7], this dataset was selected because it is the only freely available database of physiological signals for the recognition of emotions [43]. Hence, the obtained results can be considered completely unbiased and the presented methodology can be easily and fairly compared

with other algorithms. Secondly, only EEG recordings have been analyzed in the present work, thus rejecting information offered by other physiological signals, also included in the database. Nonetheless, analysis of complementary information among EEG recordings and other physiological signals requires an extensive and detailed study, which is out of the scope of this work. Anyway, given its interest, it will be addressed in the future. Lastly, it should be noted that the used visual stimuli were sufficiently long to elicit several subsequent emotions, thus making the self-assessment of their arousal and valence levels difficult. This fact could explain why the results obtained in every work using the DEAP database have been relatively low compared with other studies where experiments are tailored [32].

5. Conclusions

Quadratic sample entropy has proven to be the first single metric with the ability to discern between emotional states of calm and negative stress from EEG recordings. Indeed, this index has only reported a discriminant ability slightly lower than previous works, where a wide variety of features have been required to be combined with advanced classifiers. Moreover, this entropy-based measure has also been able to reveal significant differences in the neural activity generated by both emotional states for all the brain areas. Nonetheless, in accordance with previous findings, the highest rates of neural activation have been found in left frontal and right parietal regions. These results together with their easy interpretation make quadratic sample entropy a promising index for the recognition of negative stress as well as to gain new information about how the brain works under this emotion.

Acknowledgments: This work was partially supported by the Spanish Ministerio de Economía y Competitividad/FEDER under TIN2013-47074-C2-1-R and TIN2015-72931-EXP grants and PPII–2014–026–P from Junta de Comunidades de Castilla La Mancha.

Author Contributions: Beatriz García-Martínez and Arturo Martínez-Rodrigo conceived and designed the study, programmed the experiments and drafted the manuscript. Roberto Zangróniz Cantabrana and Jose Manuel Pastor García helped to interpret the results and reviewed the manuscript. Finally, Raúl Alcaraz supervised the experiments, reviewed the manuscript and contributed to the final version. All authors have read and approved the final version of the manuscript.

Conflicts of Interest: The authors declare no conflict of interest.

References

1. Coan, J.A.; Allen, J.J.B. *Handbook of Emotion Elicitation and Assessment*; Oxford University Press: Oxford, UK, 2007.
2. Rukavina, S.; Gruss, S.; Hoffmann, H.; Tan, J.W.; Walter, S.; Traue, H.C. Affective Computing and the Impact of Gender and Age. *PLoS ONE* **2016**, *11*, e0150584.
3. Mitchell, A.J.; Lord, K.; Slattery, J.; Grainger, L.; Symonds, P. How feasible is implementation of distress screening by cancer clinicians in routine clinical care? *Cancer* **2012**, *118*, 6260–6269.
4. Rozanski, A. Behavioral cardiology: Current advances and future directions. *J. Am. Coll. Cardiol.* **2014**, *64*, 100–110.
5. Tadic, B.; Gligorijevic, V.; Mitrovic, M.; Suvakov, M. Co-Evolutionary Mechanisms of Emotional Bursts in Online Social Dynamics and Networks. *Entropy* **2013**, *15*, 5084–5120.
6. Chanel, G.; Rebetez, C.; Bétrancourt, M.; Pun, T. Emotion Assessment From Physiological Signals for Adaptation of Game Difficulty. *IEEE Trans. Syst. Man Cybernet. Part A* **2011**, *41*, 1052–1063.
7. Valenza, G.; Lanata, A.; Scilingo, E.P. The Role of Nonlinear Dynamics in Affective Valence and Arousal Recognition. *IEEE Trans. Affect. Comput.* **2012**, *3*, 237–249.
8. Ekman, P. An argument for basic emotions. *Cognit. Emot.* **1992**, *6*, 169–200.
9. Schröder, M.; Cowie, R. Towards emotion-sensitive multimodal interfaces: The challenge of the European Network of Excellence HUMAINE. In Proceedings of the Adapting the Interaction Style to Affective Factors Workshop in Conjunction with User Modeling, Edinburgh, UK, 25 July 2005.
10. Russell, J.A. A circumplex model of affect. *J. Pers. Soc. Psychol.* **1980**, *39*, 1161–1178.

11. Calvo, R.A.; D'Mello, S.K. Affect Detection: An Interdisciplinary Review of Models, Methods, and Their Applications. *IEEE Trans. Affect. Comput.* **2010**, *1*, 18–37.
12. Kreibig, S.D. Autonomic nervous system activity in emotion: A review. *Biol. Psychol.* **2010**, *84*, 394–421.
13. Russell, J.A.; Bachorowski, J.A.; Fernandez-Dols, J.M. Facial and vocal expressions of emotion. *Annu. Rev. Psychol.* **2003**, *54*, 329–349.
14. Jenke, R.; Peer, A.; Buss, M. Feature Extraction and Selection for Emotion Recognition from EEG. *IEEE Trans. Affect. Comput.* **2014**, *5*, 327–339.
15. Mauss, I.B.; Robinson, M.D. Measures of emotion: A review. *Cognit. Emot.* **2009**, *23*, 209–237.
16. Daly, I.; Malik, A.; Hwang, F.; Roesch, E.; Weaver, J.; Kirke, A.; Williams, D.; Miranda, E.; Nasuto, S.J. Neural correlates of emotional responses to music: An EEG study. *Neurosci. Lett.* **2014**, *573*, 52–57.
17. Lee, Y.Y.; Hsieh, S. Classifying different emotional states by means of EEG-based functional connectivity patterns. *PLoS ONE* **2014**, *9*, e95415.
18. Martini, N.; Menicucci, D.; Sebastiani, L.; Bedini, R.; Pingitore, A.; Vanello, N.; Milanesi, M.; Landini, L.; Gemignani, A. The dynamics of EEG gamma responses to unpleasant visual stimuli: From local activity to functional connectivity. *NeuroImage* **2012**, *60*, 922–932.
19. Lee, T.W.; Wu, Y.T.; Yu, Y.W.Y.; Chen, M.C.; Chen, T.J. The implication of functional connectivity strength in predicting treatment response of major depressive disorder: A resting EEG study. *Psychiatry Res. Neuroimag.* **2011**, *194*, 372–377.
20. Fingelkurts, A.A.; Fingelkurts, A.A.; Rytsälä, H.; Suominen, K.; Isometsä, E.; Kähkönen, S. Impaired functional connectivity at EEG alpha and theta frequency bands in major depression. *Hum. Brain Mapp.* **2007**, *28*, 247–261.
21. Varotto, G.; Fazio, P.; Sebastiano, D.R.; Avanzini, G.; Franceschetti, S.; Panzica, F. Music and emotion: An EEG connectivity study in patients with disorders of consciousness. In Proceedings of the 2012 Annual International Conference of the IEEE Engineering in Medicine and Biology Society (EMBC), San Diego, CA, USA, 28 August–1 September 2012; pp. 5206–5209.
22. Liao, W.; Zhang, Z.; Pan, Z.; Mantini, D.; Ding, J.; Duan, X.; Luo, C.; Lu, G.; Chen, H. Altered functional connectivity and small-world in mesial temporal lobe epilepsy. *PLoS ONE* **2010**, *5*, e8525.
23. Stam, C.; Jones, B.; Nolte, G.; Breakspear, M.; Scheltens, P. Small-world networks and functional connectivity in Alzheimer's disease. *Cerebr. Cortex* **2007**, *17*, 92–99.
24. Micheloyannis, S.; Pachou, E.; Stam, C.J.; Breakspear, M.; Bitsios, P.; Vourkas, M.; Erimaki, S.; Zervakis, M. Small-world networks and disturbed functional connectivity in schizophrenia. *Schizophr. Res.* **2006**, *87*, 60–66.
25. Kim, M.K.; Kim, M.; Oh, E.; Kim, S.P. A review on the computational methods for emotional state estimation from the human EEG. *Comput. Math. Methods Med.* **2013**, *2013*, doi:10.1155/2013/573734.
26. Abásolo, D.; Hornero, R.; Gómez, C.; García, M.; López, M. Analysis of EEG background activity in Alzheimer's disease patients with Lempel-Ziv complexity and central tendency measure. *Med. Eng. Phys.* **2006**, *28*, 315–322.
27. Cao, Y.; Cai, L.; Wang, J.; Wang, R.; Yu, H.; Cao, Y.; Liu, J. Characterization of complexity in the electroencephalograph activity of Alzheimer's disease based on fuzzy entropy. *Chaos* **2015**, *25*, 083116.
28. Labate, D.; La Foresta, F.; Morabito, G.; Palamara, I.; Morabito, F.C. Entropic measures of EEG complexity in alzheimer's disease through a multivariate multiscale approach. *IEEE Sens. J.* **2013**, *13*, 3284–3292.
29. Lalonde, F.; Gogtay, N.; Giedd, J.; Vydelingum, N.; Brown, D.; Tran, B.Q.; Hsu, C.; Hsu, M.K.; Cha, J.; Jenkins, J.; *et al*. Brain order disorder 2nd group report of f-EEG. *Proc. SPIE* **2014**, *9118*, doi:10.1117/12.2051706.
30. Xiang, J.; Li, C.; Li, H.; Cao, R.; Wang, B.; Han, X.; Chen, J. The detection of epileptic seizure signals based on fuzzy entropy. *J. Neurosci. Methods* **2015**, *243*, 18–25.
31. Acharya, U.R.; Sudarshan, V.K.; Adeli, H.; Santhosh, J.; Koh, J.E.W.; Puthankatti, S.D.; Adeli, A. A Novel Depression Diagnosis Index Using Nonlinear Features in EEG Signals. *Eur. Neurol.* **2015**, *74*, 79–83.
32. Bong, S.Z.; Murugappan, M.; Yaacob, S. Methods and approaches on inferring human emotional stress changes through physiological signals: A review. *IJMEI* **2013**, *5*, 152–162.
33. Alberdi, A.; Aztiria, A.; Basarab, A. Towards an automatic early stress recognition system for office environments based on multimodal measurements: A review. *J. Biomed. Inform.* **2016**, *59*, 49–75.

34. Healey, J.; Picard, R.W. Detecting stress during real-world driving tasks using physiological sensors. *IEEE Trans. Intell. Transp. Syst.* **2005**, *6*, 156–166.
35. Skinner, M.J.; Simpson, P.A. Workload issues in military tactical airlift. *Int. J. Aviat. Psychol.* **2002**, *12*, 79–93.
36. Marrelli, M.; Gentile, S.; Palmieri, F.; Paduano, F.; Tatullo, M. Correlation between Surgeon's experience, surgery complexity and the alteration of stress related physiological parameters. *PLoS ONE* **2014**, *9*, e112444.
37. Carneiro, D.; Novais, P.; Pêgo, J.M.; Sousa, N.; Neves, J. Using Mouse Dynamics to Assess Stress During Online Exams. In Proceedings of the Hybrid Artificial Intelligent Systems—10th International Conference, HAIS 2015, Bilbao, Spain, 22–24 June 2015; pp. 345–356.
38. Martínez-Rodrigo, A.; Zangróniz, R.; Pastor, J.M.; Fernández-Caballero, A. Arousal Level Classification in the Ageing Adult by Measuring Electrodermal Skin Conductivity. In *Lecture Notes in Computer Science*; Springer: Berlin/Heidelberg, Germany, 2015; Volume 9456, pp. 213–223.
39. Bender, R.E.; Alloy, L.B. Life stress and kindling in bipolar disorder: Review of the evidence and integration with emerging biopsychosocial theories. *Clin. Psychol. Rev.* **2011**, *31*, 383–398.
40. Pickering, T.G. Mental stress as a causal factor in the development of hypertension and cardiovascular disease. *Curr. Hypertens. Rep.* **2001**, *3*, 249–254.
41. Mönnikes, H.; Tebbe, J.J.; Hildebrandt, M.; Arck, P.; Osmanoglou, E.; Rose, M.; Klapp, B.; Wiedenmann, B.; Heymann-Mönnikes, I. Role of stress in functional gastrointestinal disorders. Evidence for stress-induced alterations in gastrointestinal motility and sensitivity. *Dig. Dis.* **2001**, *19*, 201–211.
42. Brzozowski, B.; Mazur-Bialy, A.; Pajdo, R.; Kwiecien, S.; Bilski, J.; Zwolinska-Wcislo, M.; Mach, T.; Brzozowski, T. Mechanisms by which Stress Affects the Experimental and Clinical Inflammatory Bowel Disease (IBD). Role of Brain-Gut Axis. *Curr. Neuropharmacol.* **2016**, *14*, 1–9.
43. Koelstra, S.; Mühl, C.; Soleymani, M.; Lee, J.; Yazdani, A.; Ebrahimi, T.; Pun, T.; Nijholt, A.; Patras, I. DEAP: A Database for Emotion Analysis using Physiological Signals. *IEEE Trans. Affect. Comput.* **2012**, *3*, 18–31.
44. Morris, J.D. Observations SAM: The Self-Assessment Manikin—An efficient cross-cultural measurement of emotional response. *J. Advert. Res.* **1995**, *35*, 63–68.
45. Hosseini, S.A.; Khalilzadeh, M.A.; Changiz, S. Emotional stress recognition system for affective computing based on bio-signals. *J. Biol. Syst.* **2010**, *18*, 101–114.
46. Bastos Filho, T.F.; Ferreira, A.; Atencio, A.C.; Arjunan, S.P.; Kumar, D. Evaluation of feature extraction techniques in emotional state recognition. In Proceedings of the 4th International Conference on Intelligent Human Computer Interaction (IHCI), Kharagpur, India, 27–29 December 2012; pp. 1–6.
47. Pomer-Escher, A.G.; de Souza, M.D.P.; Filho, T.F.B. Methology for analysis of stress level based on asymmetry patterns of alpha rhythms in EEG signals. In Proceedings of the 5th ISSNIP-IEEE Biosignals and Biorobotics Conference: Biosignals and Robotics for Better and Safer Living (BRC), Salvador, Brazil, 26–28 May 2014; pp. 1–5.
48. Faust, O.; Bairy, M.G. Nonlinear analysis of physiological signals: A review. *J. Mech. Med. Biol.* **2012**, *12*, doi:10.1142/S0219519412400155.
49. Pincus, S.M. Approximate entropy as a measure of system complexity. *Proc. Natl. Acad. Sci. USA* **1991**, *88*, 2297–2301.
50. Richman, J.S.; Moorman, J.R. Physiological time-series analysis using approximate entropy and sample entropy. *Am. J. Physiol. Heart Circ. Physiol.* **2000**, *278*, H2039–H2049.
51. Lake, D.E.; Moorman, J.R. Accurate estimation of entropy in very short physiological time series: The problem of atrial fibrillation detection in implanted ventricular devices. *Am. J. Physiol. Heart Circ. Physiol.* **2011**, *300*, H319–H325.
52. Pincus, S.M. Assessing serial irregularity and its implications for health. *Ann. N. Y. Acad. Sci.* **2001**, *954*, 245–267.
53. Hornero, R.; Abásolo, D.; Escudero, J.; Gómez, C. Nonlinear analysis of electroencephalogram and magnetoencephalogram recordings in patients with Alzheimer's disease. *Philos. Trans. A Math. Phys. Eng. Sci.* **2009**, *367*, 317–336.
54. Costa, M.; Goldberger, A.L.; Peng, C.K. Multiscale entropy analysis of complex physiologic time series. *Phys. Rev. Lett.* **2002**, *89*, 068102.
55. Li, P.; Liu, C.; Li, K.; Zheng, D.; Liu, C.; Hou, Y. Assessing the complexity of short-term heartbeat interval series by distribution entropy. *Med. Biol. Eng. Comput.* **2015**, *53*, 77–87.

56. Jung, Y.; Jianhua, H. A *K*-fold averaging cross-validation procedure. *J. Nonparametr. Stat.* **2015**, *27*, 167–179.
57. Breiman, L. *Classification and Regression Trees*; Wadsworth International Group: Belmont, CA, USA, 1984.
58. Jolliffe, I. *Principal Component Analysis*; Wiley Online Library: Hoboken, NJ, USA, 2002.
59. Hatamikia, S.; Nasrabadi, A. Recognition of emotional states induced by music videos based on nonlinear feature extraction and SOM classification. In Proceedings of the 21th Iranian Conference on Biomedical Engineering (ICBME), Tehran, Iran, 26–28 November 2014; pp. 333–337.
60. Lu, S.; Chen, X.; Kanters, J.K.; Solomon, I.C.; Chon, K.H. Automatic selection of the threshold value *r* for approximate entropy. *IEEE Trans. Biomed. Eng.* **2008**, *55*, 1966–1972.
61. Chon, K.; Scully, C.G.; Lu, S. Approximate entropy for all signals. *IEEE Eng. Med. Biol. Mag.* **2009**, *28*, 18–23.
62. Liu, C.; Liu, C.; Shao, P.; Li, L.; Sun, X.; Wang, X.; Liu, F. Comparison of different threshold values *r* for approximate entropy: Application to investigate the heart rate variability between heart failure and healthy control groups. *Physiol. Meas.* **2011**, *32*, 167–180.
63. Lang, P.J.; Bradley, M.M.; Cuthbert, B.N. Emotion, motivation, and anxiety: Brain mechanisms and psychophysiology. *Biol. Psychiatry* **1998**, *44*, 1248–1263.
64. Begić, D.; Hotujac, L.; Jokić-Begić, N. Electroencephalographic comparison of veterans with combat-related post-traumatic stress disorder and healthy subjects. *Int. J. Psychophysiol.* **2001**, *40*, 167–172.
65. Metzger, L.J.; Paige, S.R.; Carson, M.A.; Lasko, N.B.; Paulus, L.A.; Pitman, R.K.; Orr, S.P. PTSD arousal and depression symptoms associated with increased right-sided parietal EEG asymmetry. *J. Abnorm. Psychol.* **2004**, *113*, 324–329.
66. Natarajan, K.; Acharya, U.R.; Alias, F.; Tiboleng, T.; Puthusserypady, S.K. Nonlinear analysis of EEG signals at different mental states. *Biomed. Eng. Online* **2004**, *3*, doi:10.1186/1475-925X-3-7.
67. Gao, J.; Fan, J.; Wu, B.W.Y.; Zhang, Z.; Chang, C.; Hung, Y.S.; Fung, P.C.W.; Sik, H.H. Entrainment of chaotic activities in brain and heart during MBSR mindfulness training. *Neurosci. Lett.* **2016**, *616*, 218–223.
68. Nitschke, W.H.J.B. The puzzle of regional brain activity in and anxiety: The importance of subtypes and comorbidity. *Cognit. Emot.* **1998**, *12*, 421–447.
69. Todder, D.; Levine, J.; Abujumah, A.; Mater, M.; Cohen, H.; Kaplan, Z. The quantitative electroencephalogram and the low-resolution electrical tomographic analysis in posttraumatic stress disorder. *Clin. EEG Neurosci.* **2012**, *43*, 48–53.
70. Dolcos, F.; Cabeza, R. Event-related potentials of emotional memory: Encoding pleasant, unpleasant, and neutral pictures. *Cognit. Affect. Behav. Neurosci.* **2002**, *2*, 252–263.